THE JOURNAL OF BIOLOGICAL CHEMISTRY
Vol. 279, No. 44, Issue of October 29, pp. 46073–46081, 2004
Printed in U.S.A.

Functional Non-equivalence of ATP-binding Cassette Signature Motifs in the Transporter Associated with Antigen Processing (TAP)*

Received for publication, April 12, 2004, and in revised form, August 17, 2004
Published, JBC Papers in Press, August 17, 2004, DOI 10.1074/jbc.M404042200

Min Chen, Rupert Abele, and Robert Tampé‡

From the Institute of Biochemistry, Biozentrum, Goethe-University Frankfurt, Marie-Curie-Strasse 9, D-60439 Frankfurt am Main, Germany

The transporter associated with antigen processing (TAP) is a key component of the cellular immune system. As a member of the ATP-binding cassette (ABC) superfamily, TAP hydrolyzes ATP to energize the transport of peptides from the cytosol into the lumen of the endoplasmic reticulum. TAP is composed of TAP1 and TAP2, each containing a transmembrane domain and a nucleotide-binding domain (NBD). Here we investigated the role of the ABC signature motif (C-loop) on the functional non-equivalence of the NBDs, which contain a canonical C-loop (LSGGQ) for TAP1 and a degenerate C-loop (LAAGQ) for TAP2. Mutation of the leucine or glycine (LSGGQ) in TAP1 fully abolished peptide transport. However, TAP complexes with equivalent mutations in TAP2 still showed residual peptide transport activity. To elucidate the origin of the asymmetry of the NBDs of TAP, we further examined TAP complexes with exchanged C-loops. Strikingly, the chimera with two canonical C-loops showed the highest transport rate whereas the chimera with two degenerate C-loops had the lowest transport rate, demonstrating that the ABC signature motifs control peptide transport efficiency. All single site mutants and chimeras showed similar activities in peptide or ATP binding, implying that these mutations affect the ATPase activity of TAP. In addition, these results prove that the serine of the C-loop is not essential for TAP function but rather coordinates, together with other residues of the C-loop, the ATP hydrolysis in both nucleotide-binding sites.

The transporter associated with antigen processing (TAP)[1] plays a pivotal role in the major histocompatibility complex class I antigen presentation pathway. Intracellular proteins are degraded in the cytosol predominantly by the 26/20 S proteasome, and a fraction of these cleavage products are transported by TAP into the endoplasmic reticulum lumen, where they bind to major histocompatibility complex class I molecules. Peptide-loaded major histocompatibility complex I are transported to the cell surface where the antigenic cargo is displayed to cytotoxic T-lymphocytes, which eventually eliminate infected or transformed cells (1).

TAP belongs to the ATP-binding cassette (ABC) transporter superfamily, the members of which use ATP to translocate a large variety of solutes across biological membranes (2). ABC transporters share a common structural organization with two cytosolic nucleotide-binding domains (NBDs) and two transmembrane domains. The TAP complex is a heterodimer composed of TAP1 (ABCB2) and TAP2 (ABCB3). Both subunits consist of a transmembrane domain followed by an NBD (3). The peptide-binding pocket is located in the transmembrane domain (4) and preferentially binds peptides with a length of 8–16 amino acids (5). The NBDs contain the Walker A and Walker B consensus sequences and the C-loop (ABC signature motif). The Walker A (G*X*X*G*X*G*K(S/T)) and Walker B (ΦΦΦΦD, where Φ resembles any hydrophobic amino acid) motifs are involved in ATP binding and hydrolysis. The Walker B motif is extended by a conserved glutamate (underlined) (ΦΦΦΦDE), which has been postulated to be the catalytic base for ATP hydrolysis (6). Mutation of this glutamate to glutamine results in the formation of a stable NBD dimer with a strongly reduced ATPase activity (6–8). The functional relevance of the C-loop remains, however, largely unsolved.

Peptide transport by TAP strictly requires ATP hydrolysis (9, 10), whereas peptide binding is an ATP-independent process (5, 11, 12). Peptide binding and ATP hydrolysis are nevertheless tightly coupled (13). Mutation of the highly conserved lysine in the Walker A motif of any NBD of TAP severely impairs peptide translocation, indicating that both NBDs function in peptide transport (14–16). Indeed, beryllium fluoride-trapping studies provided direct evidence that both NBDs hydrolyze ATP during peptide translocation (17). Evidence for a functional asymmetry of the NBDs of TAP came from the analysis of mutations in the Walker A motif that interrupt peptide transport when introduced in TAP2 but still show low transport activity if placed in TAP1 (14, 15, 18). Furthermore, TAP complexes with two identical NBDs translocate peptides with a drastically decreased activity, whereas TAP complexes containing switched NBDs showed wild type activity (19, 20).

Recent structural and biochemical studies demonstrated that the NBDs of ABC transporters dimerize in the presence of ATP (6–8, 21–23). Two ATPs are sandwiched at the interface between the two NBDs, positioned by the Walker A/B motifs of one NBD and the C-loop of the other NBD (Fig. 1*A*). In the dimer, the γ-phosphate of ATP is fixed by additional hydrogen bonds to the hydroxyl group of the highly conserved serine (underlined) and the amide of the invariant second glycine (underlined) of the C-loop (LSGGQ). Although these studies elucidate structural aspects of the symmetric NBD dimer for-

* This work was supported by Deutsche Forschungsgemeinschaft Grant SFB 628. The costs of publication of this article were defrayed in part by the payment of page charges. This article must therefore be hereby marked "*advertisement*" in accordance with 18 U.S.C. Section 1734 solely to indicate this fact.

‡ To whom correspondence should be addressed. Tel.: 49-69-798-29475; Fax: 49-69-798-29495; E-mail: tampe@em.uni-frankfurt.de.

[1] The abbreviations used are: TAP, transporter associated with antigen processing; ABC, ATP-binding cassette; CFTR, cystic fibrosis transmembrane conductance regulator; NBD, nucleotide-binding domain; wt, wild type.

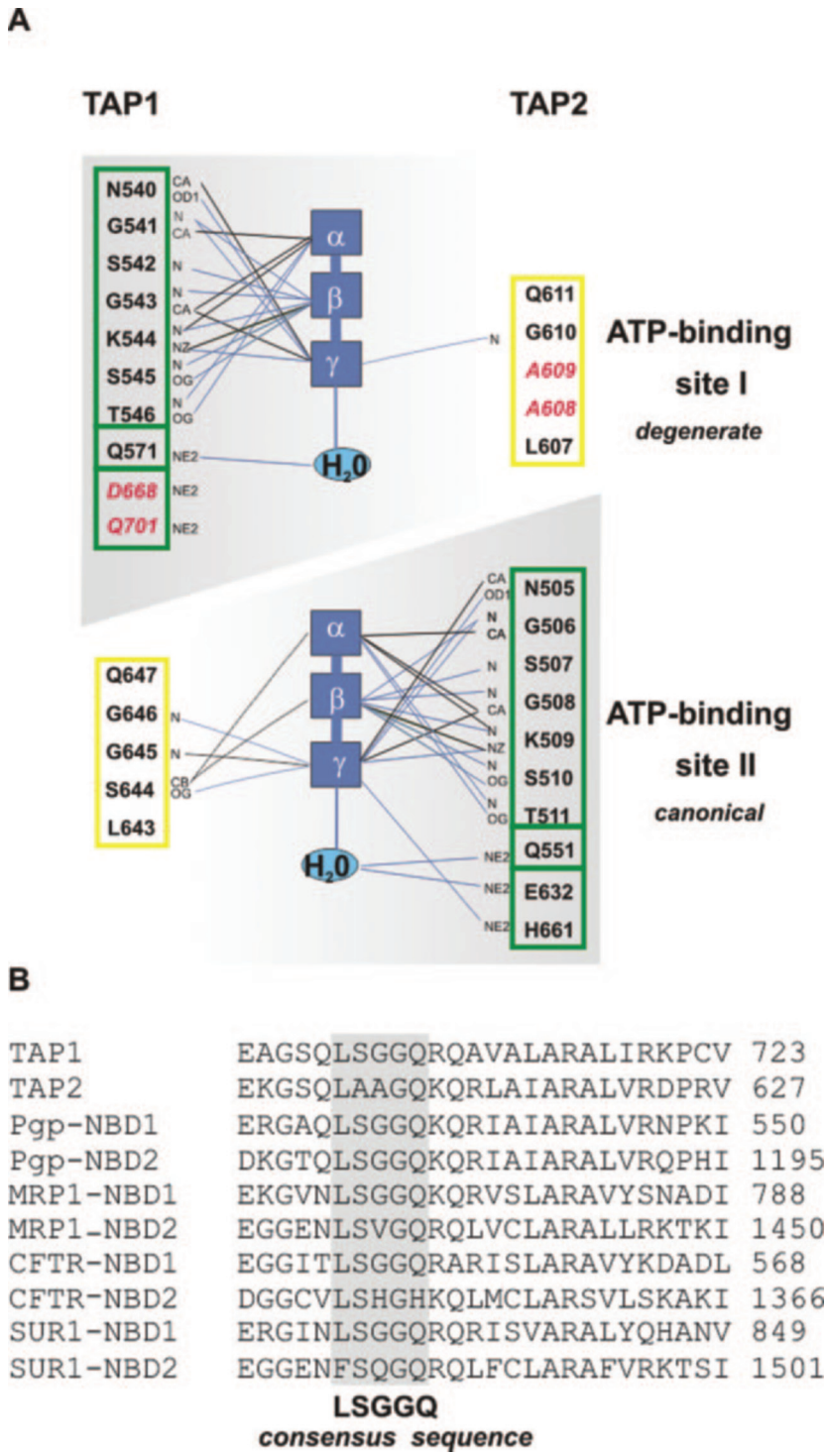

FIG. 1. **Organization of the ATP-binding sites in the TAP complex.** *A*, schematic model of the two catalytic sites in the ATP-sandwiched dimer of TAP. The Walker A motif, the putative catalytic base, and the Q- and H-loops are illustrated in *green boxes*, and the C-loop of the opposite NBD is shown in *yellow boxes*. The interaction between NBDs and phosphate groups of ATP are adopted from the structures of MJ0796 and Rad50 (6, 42). Van der Waals contacts (≤0.36 nm) are represented by *black lines*, whereas *blue lines* symbolize hydrogen bonds (≤0.33 nm). The non-conserved residues at ATP-binding site I are highlighted in *red*. Single letter amino acid abbreviations are used with position numbers. *B*, sequence alignment of the C-loops of various human ABC transporters.

mation, the functional asymmetry of the NBDs in some ABC transporters is not yet explained.

The functional non-equivalence of the two NBDs of TAP may be reflected in variations of the conserved motifs. Notably, all differences from the canonical sequences of ABC proteins affect ATP-binding site I, which, per definition, is built up by the Walker A and B motifs of TAP1 and the C-loop of TAP2. For example, the conserved glutamate (putative catalytic base) downstream of the Walker B motif in TAP1 is replaced by an aspartate, and the conserved histidine of the H-loop (switch region) of TAP1 interacting with the γ-phosphate of ATP is exchanged for glutamine (Fig. 1*A*). Most remarkably, these changes in TAP1 are coupled to alterations in the C-loop of TAP2, which is degenerate from the canonical LSGGQ sequence to LAAGQ (Fig. 1*B*). The serine in the C-loop is fully conserved among all human ABC transporters, and substitution of this residue is only found in TAP2 (Fig. 1*B*). In this study, we examined the contribution of the ABC signature motifs to the functional asymmetry of both TAP subunits by single site mutations and chimeras.

EXPERIMENTAL PROCEDURES

Materials—8-Azido-[α-^{32}P]ATP was purchased from ICN. Peptides used in this study were RRYQKSTEL (R9LQK) and RRYQNSTEL (*N*-glycosylation site is underlined). For immune detection, the monoclonal antibodies 148.3 (anti-TAP1) (24) and 435.3 (anti-TAP2) (5) and

the polyclonal antibodies 1p2 (anti-TAP1) and 2p3 (anti-TAP2) (4, 17) were used.

Baculovirus Expression Constructs—Human TAP1 was cloned into the BamHI and NotI sites of pFastBacDual (Invitrogen) under the control of the polyhedrin promoter (pFastBacDual.TAP1wt). Human TAP2 was cloned into pFastBacDual in the XhoI and SphI sites downstream of the p10 promoter (pFastBacDual.TAP2wt). Site-directed mutations (L643A, TAP1; G646V, TAP1; G646D, TAP1; L607A, TAP2; G610V, TAP2; G610D, TAP2; S644A/G645A, TAP1; and A608S/A609G, TAP2) were introduced by sequence overlapping PCR using pFastBacDual.TAP1wt or pFastBacDual.TAP2wt as templates. The sequences of the sense oligonucleotides were as follows: 5′-GCTGGGAGCCAGGCGTCAGGGGGTCAG-3′ for TAP1L643A; 5′-CAGCTGTCAGGGGTTCAGCGACAGGCAG-3′ for TAP1G646V; 5′-CAGCTGTCAGGGGATCAGCGACAGGCAG-3′ for TAP1G646D; 5′-GGAAGCCAGGCGGCTGCGGGACAGAAAC-3′ for TAP2L607A; 5′-GCTGGCTGCGGTACAGAAACAACGTC-3′ for TAP2G610V; 5′-GCTGGCTGCGGACCAGAAACAACGTCTG-3′ for TAP2G610D; 5′-GCTGGGAGCCAGCTGGCAGCGGGTCAGCGACAGGCA-3′ for TAP1S644A/G645A; and 5′-GAAGGGAAGCCAGCTGTCTGGGGGACAGAAACAACG-3′ for TAP2A608S/A609G, respectively (mutated bases are underlined). The sequences of all constructs were confirmed by DNA sequencing. Mutated TAP1 fragments were subcloned into the pFastBacDual.TAP2wt and *vice versa*, resulting in plasmids encoding both subunits (pFastBacDual.TAP1/TAP2).

Recombinant Baculovirus, Virus Infection, and Preparation of Microsomes—Recombinant bacmid DNA was produced by transformation of the DH10Bac with pFastBacDual.TAP1/TAP2 according to the manufacturer's protocol (Invitrogen). To generate recombinant baculovirus, Sf9 insect cells were transfected with 5 μg of bacmid DNA using the BaculoGold transfection kit (BD Biosciences). After 7–9 days, the supernatant was harvested and used for further amplification of the virus. TAP mutants were expressed by infection of Sf9 cells with a multiplicity of infection of 3–5. Microsomes were prepared as described previously (24).

Peptide Binding and Transport—Peptide binding to TAP was performed using filter assays and ^{125}I-labeled peptides as described previously (17). Filter plates (MultiScreen plates with glass fiber filter, pore size 1 μm; Millipore) were pre-incubated with 100 μl of 0.3% polyethylene imine followed by incubation with 100 μl of 0.2% dialyzed bovine serum albumin. Radiolabeled peptides were incubated with TAP-containing microsomes (15 μg protein) in 50 μl of AP buffer (phosphate-buffered saline buffer and 5 mM $MgCl_2$, pH 7) at 4 °C for 15 min. Microsomes were added to the filter plate and washed three times with 150 μl of ice-cold AP buffer. Radioactivity on the filters was determined by γ-counting. Background binding was determined in the presence of a 400-fold excess of unlabeled peptides. Specifically bound peptides were plotted against total peptide concentration and fitted with the Langmuir (1:1) binding equation, shown in Equation 1,

$$B = \frac{B_{max} \times [P]}{K_D + [P]} \quad \text{(Eq. 1)}$$

where B corresponds to the bound peptide, K_D is the dissociation constant, $[P]$ is the concentration of peptide, and B_{max} is the maximal amount of bound peptides. *In vitro* transport assays were performed using the peptide RRYQNSTEL as described previously (17).

8-Azido-[α-^{32}P]ATP Photo-cross-linking—Microsomes (100 μg protein) were suspended in 25 μl of transport buffer (20 mM HEPES, 140 mM NaCl, 2 mM $MgCl_2$, 5 mM NaN_3, 1 mM ouabain, 0.1 mM EGTA, and 15% glycerol, pH 7.5) containing 2.5 μM of 8-azido-[α-^{32}P]ATP. After 5 min of incubation on ice, samples were UV light-irradiated for 5 min at 4 °C. TAP was solubilized and disassembled by incubating with immunoprecipitation buffer (20 mM Tris, 150 mM NaCl, 1% Igepal, and 0.5% SDS, pH 7.5) at 37 °C for 15 min. TAP1 and TAP2 were immunoprecipitated separately by their respective antibodies, 1p2 and 2p3, and analyzed by SDS-PAGE as described previously (17). Afterward, the proteins were transferred from the gel to a nitrocellulose membrane, which was finally exposed to BIOMAX™ MS films (Kodak) with an intensifying screen at −80 °C. To check if equal amounts of TAP1 or TAP2 were immunoprecipitated, the same membranes were developed with monoclonal antibodies against TAP1 (148.3) or TAP2 (435.3). To ensure that only single subunits were immunoprecipitated, the antibodies were removed from the blot membrane by incubation for 20 min at 50 °C with stripping buffer (40 mM Tris, 2% SDS, and 100 mM β-mercaptoethanol, pH 7.5). Then, a second immunodetection was performed with polyclonal antibodies against TAP1 (1p2) or TAP2 (2p3).

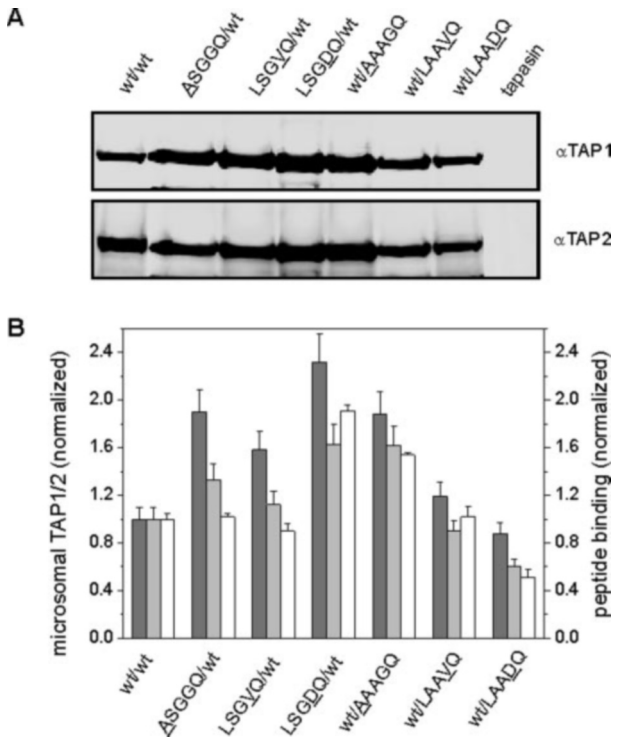

FIG. 2. **Expression and peptide binding of single site C-loop mutants.** *A*, comparison of the expression level of various C-loop mutants. Microsomes of baculovirus-infected Sf9 insect cells were analyzed by SDS-PAGE (20 μg protein per lane) followed by immunoblotting with anti-TAP1 (148.3) or anti-TAP2 (435.3) antibodies. Tapasin-expressing microsomes were used as negative control (32). *B*, correlation between expression level and peptide-binding sites. The signal intensity of each lane was scanned and analyzed by a LumiImager. The relative expression level of TAP1 (*gray*) and TAP2 (*light gray*) of each construct to wild type was determined. The amount of heterodimeric TAP complexes in microsomes (20-μg proteins) was measured by peptide binding (5 μM radiolabeled R9LQK) as described under "Experimental Procedures." The ratio between the peptide-binding sites for each construct in relation to wild type TAP was plotted (*white*). Data represent the mean of triplicate measurements, and the *error bars* represent the S.D.

RESULTS

Single Site Mutants of the C-loop—It was recently shown that the NBDs from both TAP1 and TAP2 are required for a functional TAP complex (19, 20) and that peptide binding stimulates ATP hydrolysis in both subunits (13, 17). Different transport activities of Walker A mutants indicate, however, a functional asymmetry of the two TAP subunits (14, 15, 18). TAP1 and TAP2 also show an asymmetry in their C-loops, LSGGQ *versus* LAAGQ. The serine residue and second glycine residue (underlined) of the C-loop (LSGGQ) contacting the γ-phosphate of ATP are highly conserved among members of the ABC superfamily, whereas the other positions in the C-loop are more divergent (Fig. 1). To examine the function of the different ABC signature motifs of both subunits, we first focused on the leucine and the highly conserved second glycine in the C-loop. The leucine, which is not in contact with ATP, is not as conserved as the remaining residues. In human ABC transporters, this residue is, in certain cases, replaced by bulky aromatic amino acids. Substitution of the leucine with the charged residue arginine eliminated the expression of the P-glycoprotein in Sf9 cells (25). Therefore, we exchanged this leucine with alanine, a less bulky residue, to avoid similar problems. In addition, the invariant glycine was changed to valine or aspartate, because analogous mutations in the CFTR cause cystic fibrosis (26, 27). The equivalent mutations in the P-glycoprotein, the yeast pheromone transporter Ste6p and the *Escherichia coli* maltose permease decrease or interrupt the

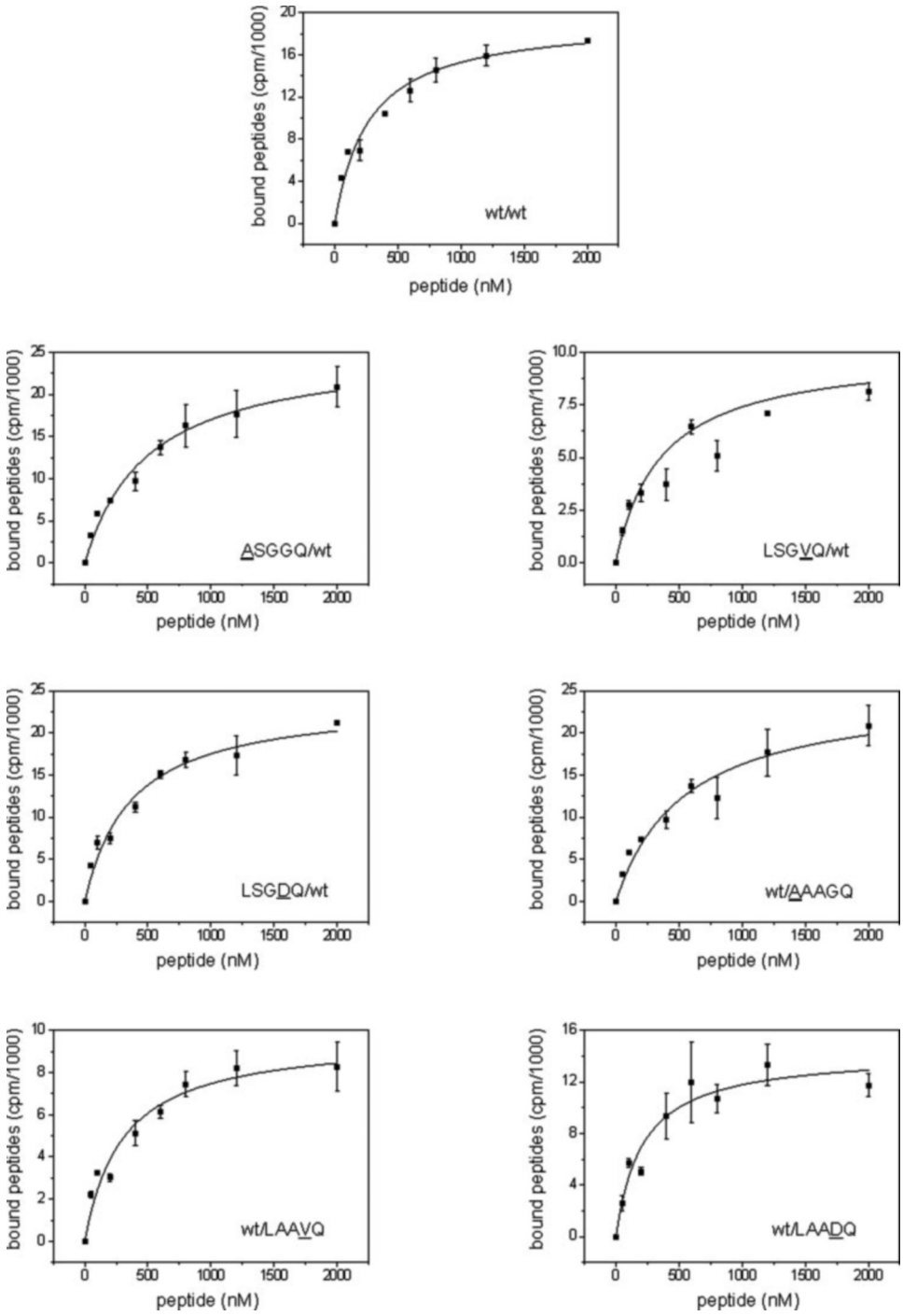

FIG. 3. **Peptide binding of single site C-loop mutants.** Peptide binding of TAP-containing microsomes (15 μg of protein) were analyzed with increasing concentrations of radiolabeled peptide R9LQK at 4 °C. Specifically bound peptides are plotted against the total peptide concentration and fitted with a Langmuir (1:1) binding equation. The peptide affinities are summarized in Table I. Data represent the mean of triplicate measurements, and the *error bars* represent the S.D.

ATPase as well as the transport activity (28–30). In our studies, all mutated half-transporters were combined with a wild type counterpart, which resulted in three pairs of mutants. These six TAP mutants are termed ASGGQ/wt *versus* wt/AAAGQ, LSGVQ/wt *versus* wt/LAAVQ, and LSGDQ/wt *versus* wt/LAADQ (mutated residues of TAP1/TAP2 are underlined). All TAP1 and TAP2 constructs were cloned into one baculovirus to circumvent the problem of double infections and expressed in Sf9 insect cells under the control of the polyhedrin and p10 promoter, respectively. Three days after infection, cells were harvested, and microsomes were isolated. The expression level of the TAP1 and TAP2 subunits and peptide binding capacity of different microsomes were analyzed and compared with the wild type protein. All of the constructs can be expressed in Sf9 cells (Fig. 2*A*). In microsomal preparations, the expression level of the various constructs varied by a factor of two. In correlation to wild type TAP, TAP1 of all mutants shows a slightly higher expression than TAP2 (Fig. 2*B*). As peptide binding of TAP requires both subunits (5, 11), we conclude that single TAP1 subunits are present in a slight excess.

Single Site Mutations in the C-loop Affect neither Peptide nor ATP Binding to TAP—Peptide binding is a prerequisite for peptide transport (5, 11), and mutations in the Walker A motif

of TAP were found to influence peptide binding at the transmembrane domain (15, 16, 18, 31). Therefore, we investigated whether these single site mutations in the C-loop have an impact on peptide binding. Binding affinities for the peptide R9LQK (RRYQKSTEL) were determined at 4 °C in the absence of ATP. As shown in Fig. 3, the data can be fitted according to a Langmuir (1:1) binding model for all TAP variants. The dissociation constant of wild type TAP was 270 nM, and all mutants showed similar peptide affinities (Table I). This finding demonstrates that the C-loop mutations do not affect the peptide-binding pocket. Because both subunits are essential for peptide binding, these results further demonstrate that these mutations do not interfere with the assembly of the heterodimeric TAP complex.

TABLE I
Peptide dissociation constants (K_D) of C-loop mutants of TAP
Mutated residues are underlined.

TAP1/TAP2	K_D
	μM
Wild type	
wt/wt	0.27 ± 0.06
Single site mutants	
ASGGQ/wt	0.50 ± 0.09
LSGVQ/wt	0.37 ± 0.13
LSGDQ/wt	0.36 ± 0.08
wt/AAAGQ	0.41 ± 0.10
wt/LAAVQ	0.30 ± 0.07
wt/LAADAQ	0.21 ± 0.06
Chimeras	
wt/LSGGQ	0.34 ± 0.02
LAAGQ/wt	0.27 ± 0.03
LAAGQ/LSGGQ	0.32 ± 0.05

We further analyzed nucleotide binding of the C-loop mutants by 8-azido-[α-^{32}P]ATP photo-cross-linking. After photo-cross-linking, the TAP complex was solubilized by Igepal and disrupted by SDS treatment. TAP1 and TAP2 were separately immunoprecipitated by polyclonal antibodies and subsequently analyzed by SDS-PAGE followed by electroblotting and autoradiography. The amount of immunoprecipitated TAP was quantified by immunodetection in combination with enhanced chemiluminiscence. By a second immunodetection with an antibody specific for the other TAP subunit, it was ensured that only one of the two subunits was analyzed by autoradiography. For TAP1, degradation products corresponding to mini7TAP were visible (32). All TAP variants bound 8-azido-[α-^{32}P]ATP, which was competed out by an excess of ATP (Fig. 4). As the binding studies were performed at the K_D of 8-azido-ATP (33),

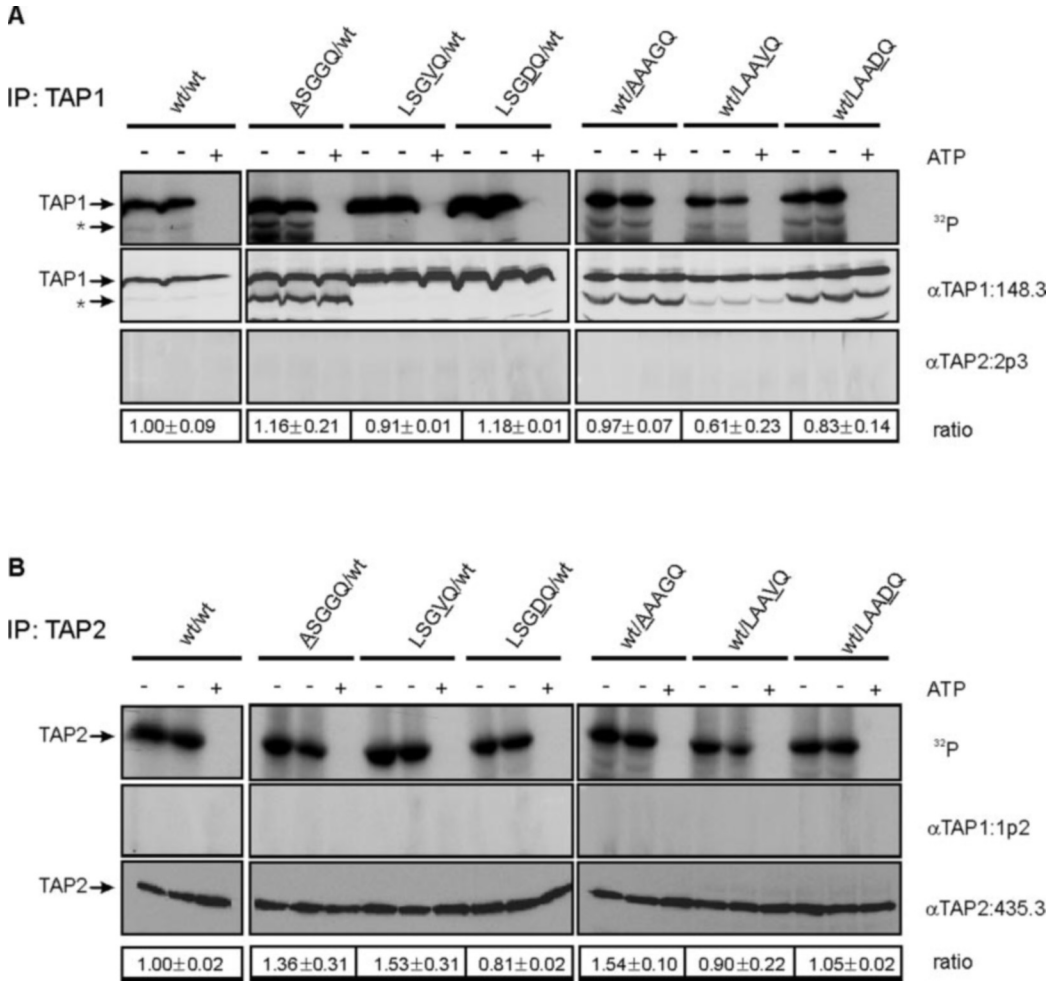

FIG. 4. **ATP binding to single site C-loop mutants.** TAP-containing microsomes (100 μg protein) were incubated with 8-azido-[α-^{32}P]ATP (2.5 μM) in the absence or the presence of 1 mM ATP at 4 °C. 8-azido-[α-^{32}P]ATP was cross-linked by UV irradiation. Subsequently, TAP complexes were solubilized and disrupted by SDS. TAP1 (*A*) and TAP2 (*B*) were immunoprecipitated (*IP*) separately with polyclonal antibodies recognizing TAP1 (1p2) or TAP2 (2p3) and separated by SDS-PAGE. Proteins were then transferred to nitrocellulose membranes, which were dried and subjected to autoradiography. To control immunoprecipitation efficiency, the same blot was also developed with monoclonal TAP1 or TAP2 antibodies (148.3 or 435.3). The membrane was redeveloped with polyclonal antibody (1p2 or 2p3) to exclude the coimmunoprecipitation of both subunits. Samples without ATP competition were duplicated to illustrate the experimental error of each experiment. The signal ratios between the autoradiogram and the immunoblot were determined and normalized to wild type TAP. Degradation products of TAP1 corresponding to mini7TAP1 (32) are marked by a *star* in *panel A*.

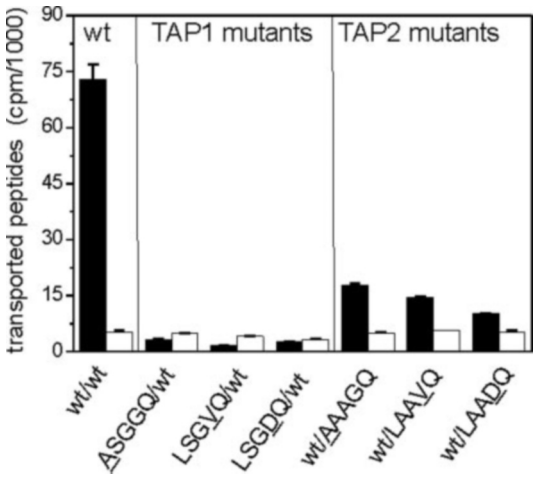

FIG. 5. **Peptide transport of single site C-loop mutants.** TAP-containing microsomes (100 μg of protein) were incubated for 5 min with 1 μM radiolabeled RRYQNSTEL in the presence of 3 mM ATP (*black*) or 3 mM ADP (*white*) at 32 °C. Glycosylated peptides were recovered by concanavalin A-Sepharose, and the radioactivity was quantified via γ-counting. Data represent the mean of triplicate measurements, and the *error bars* represent the S.D.

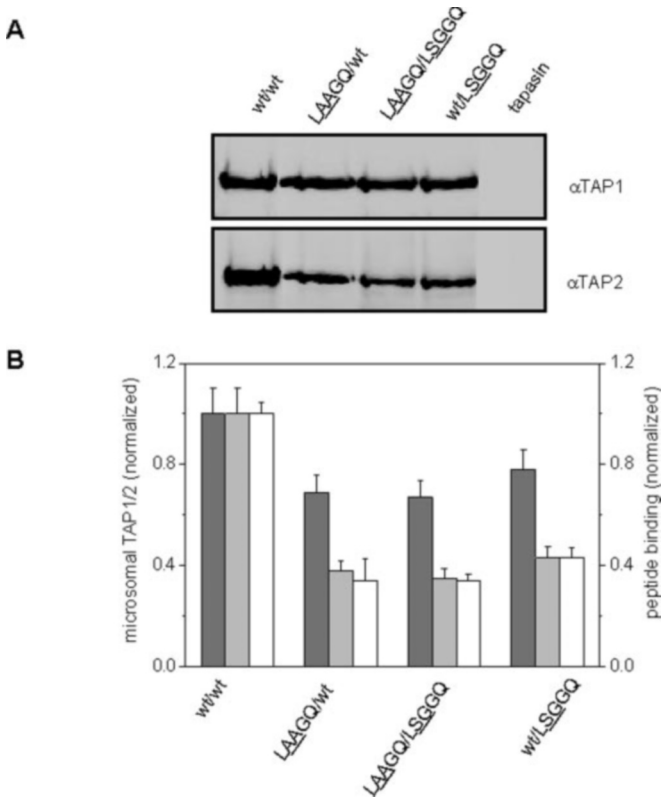

FIG. 6. **Expression and peptide binding of C-loop chimeras.** *A*, comparison of the expression level of various C-loop chimeras. Microsomes of baculovirus-infected Sf9 insect cells were analyzed by SDS-PAGE (20 μg of protein per lane) and immunoblotting with anti-TAP1 (148.3) or anti-TAP2 (435.3) antibodies. Tapasin-expressing microsomes were used as a negative control. *B*, correlation between the expression level and the peptide binding sites. The signal intensity of each lane was scanned and analyzed by a LumiImager. The relative expression level of TAP1 (*gray*) and TAP2 (*light gray*) of each construct to wild type was determined. The amount of heterodimeric TAP complexes in microsomes (20 μg of protein) was measured by peptide binding (5 μM radiolabeled R9LQK) as described under "Experimental Procedures." The ratio between the peptide-binding sites for each construct in relation to wild type TAP was plotted (*white*). Data represent the mean of triplicate measurements, and the *error bars* represent the S.D.

the influence of the mutations on ATP binding can be directly studied by comparing the ratio of ATP photo-cross-linking to immunoprecipitated TAP1 or TAP2. As shown in Fig. 4, the normalized ratios for all C-loop TAP mutants are very similar. In summary, we concluded that these single site mutations do not influence ATP binding to TAP. This is in agreement with studies on single TAP subunits and TAP complexes, all showing similar affinities for ATP in the micromolar range (33).

Single Site Mutations of the C-loop Severely Affect Peptide Transport—All described C-loop mutants had no significant effect on peptide or ATP binding. Finally, the peptide transport activity of these C-loop mutants was investigated. *In vitro* peptide transport assays were performed as described using TAP-containing microsomes and the radiolabeled peptide RRYQNSTEL (9, 24). In these experiments, the TAP concentration determined by immunoblotting was kept constant. In contrast to wild type TAP, we did not observe any transport activity for all mutants over a period of 2 min. Thus, the transport assay was extended to 5 min. Even under these prolonged transport periods all TAP complexes containing TAP1 mutants remained inactive (Fig. 5). In contrast, TAP complexes with mutated TAP2 transported peptides, albeit with much lower efficiency than wild type TAP. As these TAP mutants showed no difference in peptide or ATP binding, the loss of function must be related to disabled ATP hydrolysis.

A Shift from the Canonical to the Degenerate C-loop Slows Down the ATP Hydrolysis—Based on the fact that the equivalent C-loop mutations in TAP1 and TAP2 described to date behaved differently, we focused on residues of the ABC signature motif that differ in TAP1 and TAP2 (LSGGQ *versus* LAAGQ). We studied TAP complexes containing two canonical C-loops (LSGGQ(wt)/LSGGQ), switched C-loops (LAAGQ/LSGGQ), or two degenerate C-loops (LAAGQ/LAAGQ(wt); mutated residues are underlined). Microsomes were prepared from insect cells infected with a recombinant baculovirus. The expression levels of all C-loop chimeras are similar, although the TAP2 levels in the mutated TAP complex were reduced in comparison to wild type (Fig. 6). We then studied the peptide binding of the C-loop chimeras using the same procedure as described above. The slightly reduced peptide-binding capacity of the TAP mutants correlates with the decreased TAP2 level (Fig. 6*B*), because only heterodimers of TAP1 and TAP2 can bind peptides (5, 11). However, all C-loop chimeras bind peptides with a similar affinity as that of wild type (Fig. 7 and Table I), demonstrating that the degenerate C-loop does not affect peptide binding.

Next, we studied ATP binding to the C-loop chimera by 8-azido-[α-^{32}P]ATP photo-cross-linking as explained for the single site mutants. All chimeras show similar ATP photolabeling as wild type TAP. The cross-linking is specific, as no signal was detected in presence of ATP (1 mM). The normalized ratios of the cross-linked and immunodetected TAP subunits demonstrate that the ATP-binding properties of all chimeras are not significantly different from those of wild type TAP. Therefore, we conclude that all C-loop chimeras bind ATP to similar extent and with similar affinities as wild type TAP (Fig. 8).

We finally investigated the peptide transport activity of the C-loop chimeras. Interestingly, unlike the single site mutants described above, all chimeras of the ABC signature motif are highly active in peptide translocation into the endoplasmic reticulum lumen. To detect even subtle differences in translocation activity, initial transport rates were analyzed (Fig. 9). The concentration of TAP determined by peptide binding (B_{max} value) was kept constant in all experiments (maximal error of $\pm$0.06% (n = 6); Table II). ATP-dependent peptide translocation into microsomes is peptide-specific and increases linearly over a period of 3 min for all TAP variants. The TAP complex

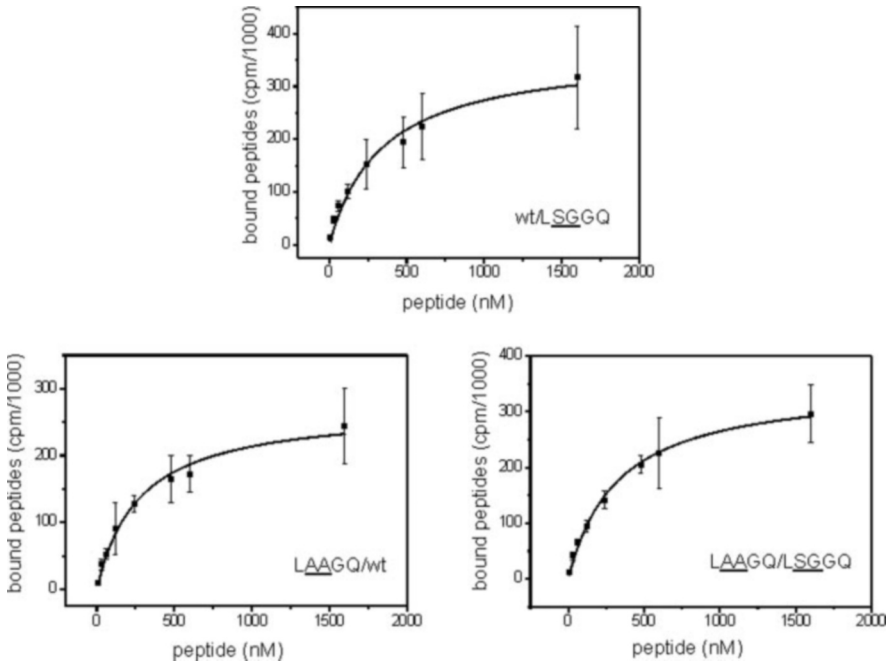

FIG. 7. **Peptide binding of the C-loop chimeras.** Peptide binding of TAP-containing microsomes (15 μg protein) were analyzed with increasing concentration of radiolabeled peptide R9LQK at 4 °C. Specifically bound peptides are plotted against the total peptide concentration and fitted with a Langmuir (1:1) binding equation. The peptide affinities are summarized in Table I. Data represent the mean of triplicate measurements and the error bars represent the S.D.

with two canonical C-loops (LSGGQ/L*SG*GQ) transports peptides with the fastest rate (115% activity in comparison to wild type TAP; Table II). The TAP chimera harboring the exchanged C-loops translocates peptides almost as efficiently as wild type TAP (91% activity). The most drastic effect was observed for the TAP complex with two degenerate C-loops with a 50% reduced transport rate. These results indicate that the C-loop in both TAP subunits controls the peptide transport rate by tuning the ATP hydrolysis in both ATP-binding sites.

DISCUSSION

Recent studies have provided the first evidence that both subunits act asymmetrically in the transport cycle of the TAP complex (14–16,18). However, the origin for this functional non-equivalence is still an open question. Therefore, we investigated the contribution of the ABC signature motif to the functional asymmetry of the TAP subunits by single site mutants and chimeras of the C-loop.

Single site mutations of the C-loop in TAP1 or TAP2 affect TAP function to a different degree, reflecting the asymmetry of both TAP subunits. Exchanging the leucine or glycine (underlined) (LSGGQ) in TAP1 fully abolished peptide transport. However, TAP complexes with equivalent mutations in TAP2 (LAAGQ) still showed residual peptide transport. Accordingly, mutations in ATP-binding site I (formed by Walker A and B motifs of TAP1 and C-loop of TAP2) are tolerated to a certain extent, whereas TAP complexes with the same mutations in site II are inactive. These findings are in harmony with studies on TAP complexes containing Walker A mutations in TAP1 (site I), which are still able to transport peptides although with very low efficiency, whereas equivalent mutations at site II fully disrupt peptide translocation (15, 33). Notably, all C-loop mutants are active in peptide and ATP binding, indicating that these mutations influence the ATPase activity of TAP. These results are supported by the recent finding that an exchange of the invariant glycine to alanine in the C-loop of TAP1 does not influence peptide binding but abrogates peptide transport via the TAP complex (34). In addition, analogous P-glycoprotein mutants of the invariant glycine in the N- or C-terminal NBD show ATP binding, but not ATPase activity (35). Furthermore, in the maltose permease (MalK), the pheromone transporter Ste6p, and the CFTR, the exchange of the invariant glycine decreases the ATPase as well as transport activity (28–30, 37). Thus, substitution of the invariant glycine of the C-loop (LSGGQ) reduces the ATPase activity of all the ABC transporters studied to date. However, there are some subtle differences, which are marked by either a total loss or a strong decrease in catalytic activity. TAP mutants of the invariant glycine are non-equivalent, implying that the degenerate ATP-binding site I is less crucial for the transport function than is site II. The C-loop mutants of TAP2 (site I) may be able to form an NBD dimer but with a strongly decreased ATPase activity. The equivalent mutation in TAP1 (site II) leads to an inactive transport complex. This model is supported by mutagenesis studies of GlcV, the NBD of the glucose transporter of *Sulfolobus solfataricus*, where mutation of the invariant second glycine in the C-loop (G144A) or mutation of the putative catalytic base (E166A) results in inactive proteins (38). Mixtures of both GlcV mutants retain, compared with wild type GlcV, ~20% ATPase activity, demonstrating that one active ATP-binding site is sufficient for ATP hydrolysis. This observation is in line with the non-equivalence of the NBDs described for CFTR and MRP1. In both ABC transporters, NBD1 binds ATP but hydrolyzes it only poorly. NBD2 possesses a strong ATPase activity and seems to be regulated by the nucleotide loading state of NBD1 (39–41). However, TAP works differently, as both subunits show a peptide-stimulated ATPase activity (17).

To decipher the origin of the asymmetry of the NBDs of TAP, we exchanged the C-loops of TAP1 and TAP2. Comparable with the single site mutants, all C-loop chimeras showed similar peptide and ATP binding activities. Strikingly, the C-loop controls the peptide transport efficiency; the chimera with two canonical C-loops showed the highest transport rate, whereas the chimera with two degenerate C-loops has the lowest transport rate. TAP complexes with mixed C-loops transport peptides with almost identical efficiency. Based on the crystal structures of NBD dimers (6, 21, 42), it was postulated that the serine of the C-loop forming a hydrogen bond to the γ-phosphate of ATP is essential for the function of ABC proteins. This serine is conserved in all human ABC proteins, except for TAP2. However, here we provide evidence that this serine is also not essential for TAP function. This observation is also supported by beryllium fluoride-trapping experiments, which

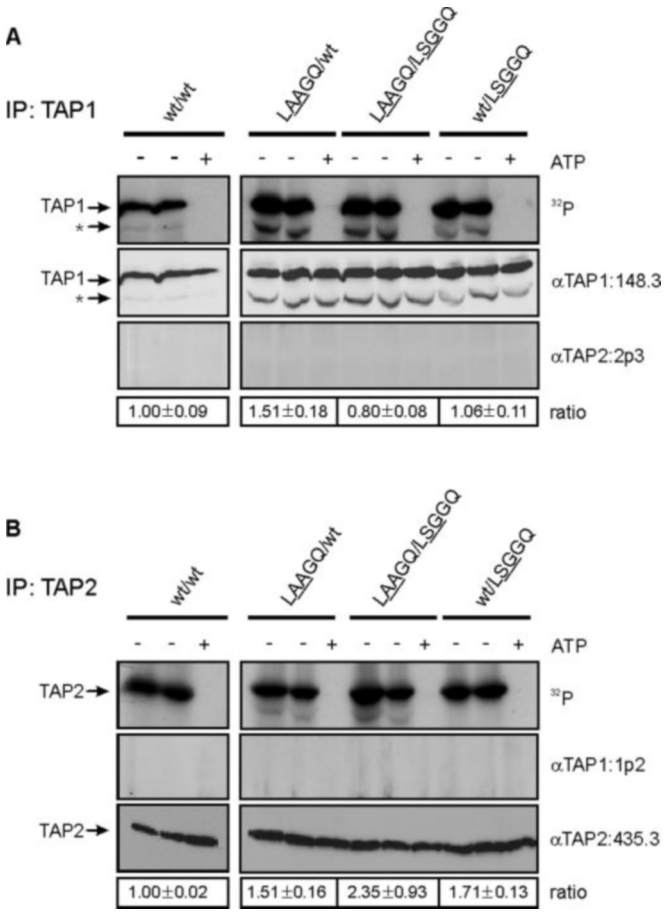

FIG. 8. **ATP binding to C-loop chimeras.** TAP-containing microsomes (100 μg of protein) were incubated with 8-azido-[α-^{32}P]ATP (2.5 μM) in the absence or the presence of 1 mM ATP at 4 °C. 8-azido-[α-^{32}P]ATP was cross-linked by UV irradiation. Subsequently, TAP complexes were solubilized and disrupted by SDS. TAP1 (*A*) and TAP2 (*B*) were immunoprecipitated (*IP*) separately with polyclonal antibodies recognizing TAP1 and TAP2 (1p2 and 2p3) and separated by SDS-PAGE. Proteins were then transferred to nitrocellulose membranes, which were dried and subjected to autoradiography. To control the immunoprecipitation efficiency, the same blot was also developed with monoclonal TAP1 (148.3) or TAP2 antibodies (435.3). The membrane was redeveloped with polyclonal antibody (1p2 or 2p3) to exclude the coimmunoprecipitation of both subunits. The samples without ATP competition were duplicated to illustrate the experimental error of each experiment. The ratio of the signal of the autoradiography and the Western-blot signal was determined and normalized to wild type TAP. Degradation products of TAP1 corresponding to mini7TAP1 (32) are marked by a *star* in *panel A*.

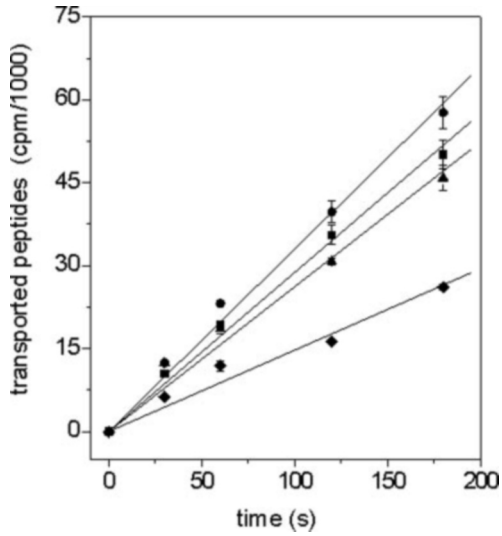

FIG. 9. **Transport kinetics of C-loop chimeras.** Microsomes corresponding to equal TAP concentrations were incubated with the radiolabeled peptide RRYQNSTEL (1 μM) in the presence of 3 mM ATP or 3 mM ADP at 32 °C. Glycosylated peptides were recovered by concanavalin A-Sepharose after different times and quantified by γ-counting. The slopes (linear fit) reflect the initial transport rates, which are listed in Table II. Each data point represents the mean of triplicate measurements (±S.D.). Similar results were obtained in three independent experiments. *Circles*, wt/LSGGQ; *squares*, wt/wt; *triangles*, LAAGQ/LSGGQ; *diamonds*, LAAGQ/wt.

TABLE II
Peptide transport rates of C-loop chimeras (underlined) of TAP

TAP1/TAP2	*k*	Error in B_{max}[a]
	cpm/1000/s	*%*
LSGGQ/LAAGQ	0.287 ± 0.007	±0.0036
LSGGQ/LSGGQ	0.330 ± 0.010	±0.0297
LAAGQ/LSGGQ	0.262 ± 0.012	±0.0613
LAAGQ/LAAGQ	0.147 ± 0.008	±0.0424

[a] $n = 6$.

demonstrated that both ATP-binding sites of TAP hydrolyze ATP in a peptide-specific manner, although the C-loop of TAP2 (site I) does not contain a serine residue (17).

The serine of the canonical C-loop may be at least partially involved in the timing of ATP hydrolysis in both nucleotide-binding sites and, hence, the asymmetry of TAP1 and TAP2. Similar findings were most recently observed for P-glycoprotein (36). Mutation of the serine in one of the C-loops of P-glycoprotein to alanine in each NBD reduces ATPase activity to 66%, and the double mutant possesses 3% of the ATPase activity of wild type P-glycoprotein. In GlcV, the serine of the C-loop was found not to be essential for ATP hydrolysis (38). The S142A mutant hydrolyzes ATP with 50% of the activity of wild type GlcV. Mutation of this serine residue to asparagine, isoleucine, or arginine in the ATP-binding site II of CFTR results in cystic fibrosis (26, 27). The same mutations in pheromone transporter Ste6p drastically reduce secretion of the mating a-factor in yeast (29). Also, the conservative exchange, serine to cysteine, reduces the ATPase activity of P-glycoprotein to 22% that of wild type P-glycoprotein (22). The glycine residue (underlined) (LSGGQ) is expected to have minor effects on the asymmetry, because this residue is divergent not only in human ABC transporters (Fig. 1) but also between human (LAAGQ) and rodent (LAVGQ) TAP2.

The TAP mutants described herein provide important information about the architecture of the C-loops in TAP. Exchange of the highly conserved glycine of the C-loop (LSGGQ) has severe effects on the transport activity. The monomeric structure of the GlcV mutant (G144A) shows, within a resolution of 0.15 nm, no conformational changes in the C-loop (38). By modeling the GlcV (G144A) dimer on the dimeric MJ0796 structure, it became evident that the methyl group of alanine causes steric hindrance with an oxygen of the γ-phosphate of ATP as well as the side chain of serine in the Walker A motif of the opposite NBD (38). Therefore, introducing any side chain at the position of the invariant glycine of the C-loop is believed to inhibit NBD dimer formation by steric hindrance. In the C-loop, the hydroxyl group of the serine forms a hydrogen bond with the γ-phosphate of ATP (6, 21). The introduction of an alanine at this position seems to strengthen the NBD dimer affinity, because, in contrast to wild type GlcV, transient GlcV dimers of S142A mutants could be detected by gel filtration in the presence of MgATP (38). This finding supports the idea that the serine to alanine mutation in the C-loop reduces the ATPase activity, which prolongs dimer formation. Accordingly, we suggest that the peptide transport rate of TAP containing

two degenerate C-loops is lowered by decreasing the rate of ATP hydrolysis and not that of NBD dimer assembly. The leucine of the C-loop points to a hydrophobic, buried environment. These hydrophobic interactions seem to stabilize the structure of the C-loop, as introducing alanine instead of leucine drastically decreases the peptide transport activity of TAP.

In summary, the C-loop is an essential motif involved in the communication between and the functional asymmetry of both subunits of the TAP complex. The substitutions of the invariant glycine or the leucine of the C-loop demonstrated the asymmetric behavior of both ATP-binding sites. These findings reveal that the ATP-binding site II is more important for the catalytic activity of TAP than is site I. The serine residue in the C-loop is not essential for transport function. Moreover, the serine to alanine substitution induces an asymmetric behavior of both NBDs potentially by slowing down the ATP hydrolysis rate. This may result in a prolonged NBD dimer formation.

Acknowledgments—We thank Eckhard Linker and Gudrun Illig for excellent technical assistance and Dr. Chris van der Does for helpful comments on the manuscript.

REFERENCES

1. Grommé, M., and Neefjes, J. (2002) *Mol. Immunol.* **39,** 181–202
2. Higgins, C. F. (2001) *Res. Microbiol.* **152,** 205–210
3. Abele, R., and Tampé, R. (1999) *Biochim. Biophys. Acta* **1461,** 405–419
4. Nijenhuis, M., and Hämmerling, G. J. (1996) *J. Immunol.* **157,** 5467–5477
5. van Endert, P. M., Tampé, R., Meyer, T. H., Tisch, R., Bach, J. F., and McDevitt, H. O. (1994) *Immunity* **1,** 491–500
6. Smith, P. C., Karpowich, N., Millen, L., Moody, J. E., Rosen, J., Thomas, P. J., and Hunt, J. F. (2002) *Mol. Cell* **10,** 139–149
7. Moody, J. E., Millen, L., Binns, D., Hunt, J. F., and Thomas, P. J. (2002) *J. Biol. Chem.* **277,** 21111–21114
8. Janas, E., Hofacker, M., Chen, M., Gompf, S., van der Does, C., and Tampé, R. (2003) *J. Biol. Chem.* **278,** 26862–26869
9. Neefjes, J. J., Momburg, F., and Hämmerling, G. J. (1993) *Science* **261,** 769–771
10. Shepherd, J. C., Schumacher, T. N., Ashton-Rickardt, P. G., Imaeda, S., Ploegh, H. L., Janeway, C. A., Jr., and Tonegawa, S. (1993) *Cell* **74,** 577–584
11. Androlewicz, M. J., and Cresswell, P. (1994) *Immunity* **1,** 7–14
12. Uebel, S., Meyer, T. H., Kraas, W., Kienle, S., Jung, G., Wiesmüller, K. H., and Tampé, R. (1995) *J. Biol. Chem.* **270,** 18512–18516
13. Gorbulev, S., Abele, R., and Tampé, R. (2001) *Proc. Natl. Acad. Sci. U. S. A.* **98,** 3732–3737
14. Lapinski, P. E., Neubig, R. R., and Raghavan, M. (2001) *J. Biol. Chem.* **276,** 7526–7533
15. Karttunen, J. T., Lehner, P. J., Gupta, S. S., Hewitt, E. W., and Cresswell, P. (2001) *Proc. Natl. Acad. Sci. U. S. A.* **98,** 7431–7436
16. Saveanu, L., Daniel, S., and van Endert, P. M. (2001) *J. Biol. Chem.* **276,** 22107–22113
17. Chen, M., Abele, R., and Tampé, R. (2003) *J. Biol. Chem.* **278,** 29686–29692
18. Alberts, P., Daumke, O., Deverson, E. V., Howard, J. C., and Knittler, M. R. (2001) *Curr. Biol.* **11,** 242–251
19. Daumke, O., and Knittler, M. R. (2001) *Eur. J. Biochem.* **268,** 4776–4786
20. Arora, S., Lapinski, P. E., and Raghavan, M. (2001) *Proc. Natl. Acad. Sci. U. S. A.* **98,** 7241–7246
21. Chen, J., Lu, G., Lin, J., Davidson, A. L., and Quiocho, F. A. (2003) *Mol. Cell* **12,** 651–661
22. Loo, T. W., Bartlett, M. C., and Clarke, D. M. (2002) *J. Biol. Chem.* **277,** 41303–41306
23. Fetsch, E. E., and Davidson, A. L. (2002) *Proc. Natl. Acad. Sci. U. S. A.* **99,** 9685–9690
24. Meyer, T. H., van Endert, P. M., Uebel, S., Ehring, B., and Tampé, R. (1994) *FEBS Lett.* **351,** 443–447
25. Bakos, E., Klein, I., Welker, E., Szabo, K., Muller, M., Sarkadi, B., and Varadi, A. (1997) *Biochem. J.* **323,** 777–783
26. Cutting, G. R., Kasch, L. M., Rosenstein, B. J., Zielenski, J., Tsui, L. C., Antonarakis, S. E., and Kazazian, H. H., Jr. (1990) *Nature* **346,** 366–369
27. Kerem, B. S., Zielenski, J., Markiewicz, D., Bozon, D., Gazit, E., Yahav, J., Kennedy, D., Riordan, J. R., Collins, F. S., Rommens, J. M., and Tsui, L. C. (1990) *Proc. Natl. Acad. Sci. U. S. A.* **87,** 8447–8451
28. Panagiotidis, C. H., Reyes, M., Sievertsen, A., Boos, W., and Shuman, H. A. (1993) *J. Biol. Chem.* **268,** 23685–23696
29. Browne, B. L., McClendon, V., and Bedwell, D. M. (1996) *J. Bacteriol.* **178,** 1712–1719
30. Ketchum, C. J., Schmidt, W. K., Rajendrakumar, G. V., Michaelis, S., and Maloney, P. C. (2001) *J. Biol. Chem.* **276,** 29007–29011
31. Knittler, M. R., Alberts, P., Deverson, E. V., and Howard, J. C. (1999) *Curr. Biol.* **9,** 999–1008
32. Koch, J., Guntrum, R., Heintke, S., Kyritsis, C., and Tampé, R. (2004) *J. Biol. Chem.* 279, 10142–10147
33. Lapinski, P. E., Raghuraman, G., and Raghavan, M. (2003) *J. Biol. Chem.* **278,** 8229–8237
34. Hewitt, E. W., and Lehner, P. J. (2003) *Eur. J. Immunol.* **33,** 422–427
35. Szakacs, G., Ozvegy, C., Bakos, E., Sarkadi, B., and Varadi, A. (2001) *Biochem. J.* **356,** 71–75
36. Tombline, G., Bartholomew, L., Gimi, K., Tyndall, G. A., and Senior, A. E. (2004) *J. Biol. Chem.* **279,** 5363–5373
37. Li, C., Ramjeesingh, M., Wang, W., Garami, E., Hewryk, M., Lee, D., Rommens, J. M., Galley, K., and Bear, C. E. (1996) *J. Biol. Chem.* **271,** 28463–28468
38. Verdon, G., Albers, S. V., van Oosterwijk, N., Dijkstra, B. W., Driessen, A. J., and Thunnissen, A. M. (2003) *J. Mol. Biol.* **334,** 255–267
39. Gao, M., Cui, H. R., Loe, D. W., Grant, C. E., Almquist, K. C., Cole, S. P., and Deeley, R. G. (2000) *J. Biol. Chem.* **275,** 13098–13108
40. Nagata, K., Nishitani, M., Matsuo, M., Kioka, N., Amachi, T., and Ueda, K. (2000) *J. Biol. Chem.* **275,** 17626–17630
41. Aleksandrov, L., Aleksandrov, A. A., Chang, X. B., and Riordan, J. R. (2002) *J. Biol. Chem.* **277,** 15419–15425
42. Höpfner, K. P., Karcher, A., Shin, D. S., Craig, L., Arthur, L. M., Carney, J. P., and Tainer, J. A. (2000) *Cell* **101,** 789–800